Appendix

PTP-MEG2 regulates quantal size and fusion pore opening through two distinct structural bases and substrates

Yun-Fei Xu et al.

CATALOGUE

Appendix Figure S1

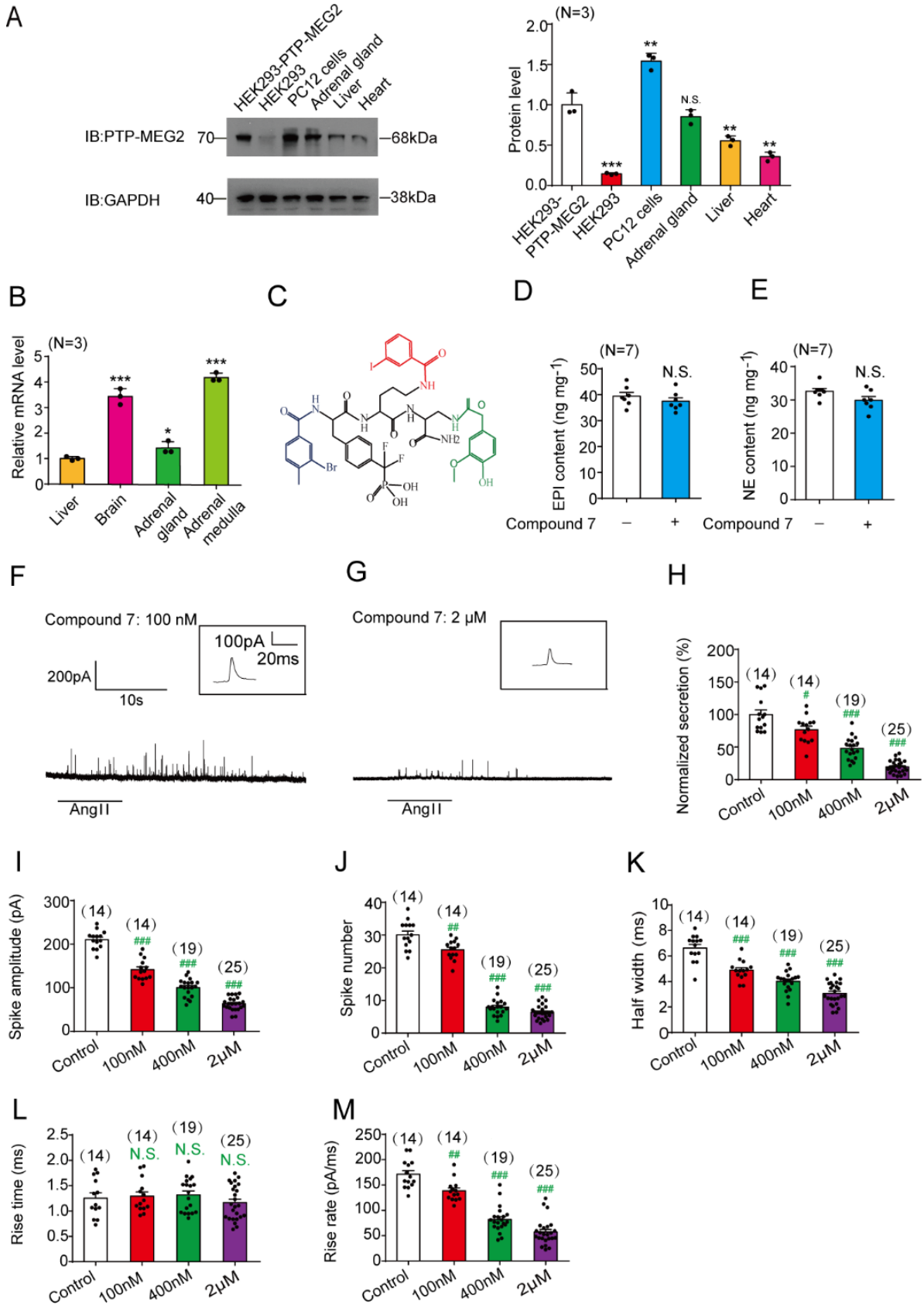

Appendix Figure S1. Inhibition of PTP-MEG2 impairs epinephrine and norepinephrine secretion.

(A). Levels of PTP-MEG2 protein expression in different cell lines and tissues by western blot. Left panel: Representative western blot was shown for the PTP-MEG2 expression in PTP-MEG2 transfected HEK-293 cells, control HEK-293 cells, PC12 cells, mouse adrenal gland, liver and heart, with GAPDH as an internal control. Right panel: Bar graph representation of the expression of PTP-MEG2 in different cell lines and tissues.

(B). PTP-MEG2 mRNA levels in mouse liver, brain, adrenal gland, and adrenal medulla were determined by quantitative reverse transcription PCR (qRT-PCR). The differences of cycle threshold values (C_T) between the samples (ΔC_T) were calculated after ratio to control GAPDH and normalized with liver expression.

(C). Schematic representation of structure of the specific PTP-MEG2 inhibitor (Compound 7) used in the manuscript.

(D-E). Total amount of EPI (epinephrine) (D) and NE (norepinephrine) (E) in isolated adrenal medulla were detected with ELISA with or without Compound 7 (400 nM) incubation for 1 hours. PTP-MEG2 inhibitor Compound 7 had no significant effects on total amounts of EPI or NE contents in adrenal medulla.

(F-G). Amperometric spikes of primary mouse chromaffin cells induced by AngII (100nM) were determined by electrochemical experiments after incubation with PTP-MEG2 inhibitor at different concentrations of 100nM (F) or 2μM (G).

(H).Statistical diagram of secretory amount of catecholamine from cells incubated with different doses of PTP-MEG2 inhibitor. The average secretory amount of cells without inhibitor was set as 100% and secretory amounts of other subgroups were normalized by ratio to control group.

(I-M). Quantitative analysis of the amperometric spikes stimulated by AngII (100nM) with or without PTP-MEG2 inhibitor at different concentrations, including the spike amplitude (I), spike number (J), half width (K), rise time (L) and rise rate (M). A total of 507 amperometric spikes were analysed from 72 chromaffin cells.

Data information: * in (A) indicates protein expression level of PTP-MEG2 in different tissues or cells compared with overexpression of PTP-MEG2 in HEK293 cells. * in (B) indicates mRNA expression level of PTP-MEG2 in different tissues compared with that in liver. # in (H-M) indicates the PTP-MEG2 inhibitor group compared with the control group. *, $P<0.05$; **, $P<0.01$; *** $P<0.001$ and #, $P<0.05$; ##, $P<0.01$; ### $P<0.001$. The bars represent mean ± s.e.m. The replicates number (N) is indicated in the graphs and refers to independent experiments in all panels. (H-M) Data were from 8 independent experiments. (D), (E), the data were analysed using Student's t-test. (A), (B) and from (H) to (M), the data were analysed using one-way ANOVA.

Appendix Figure S2

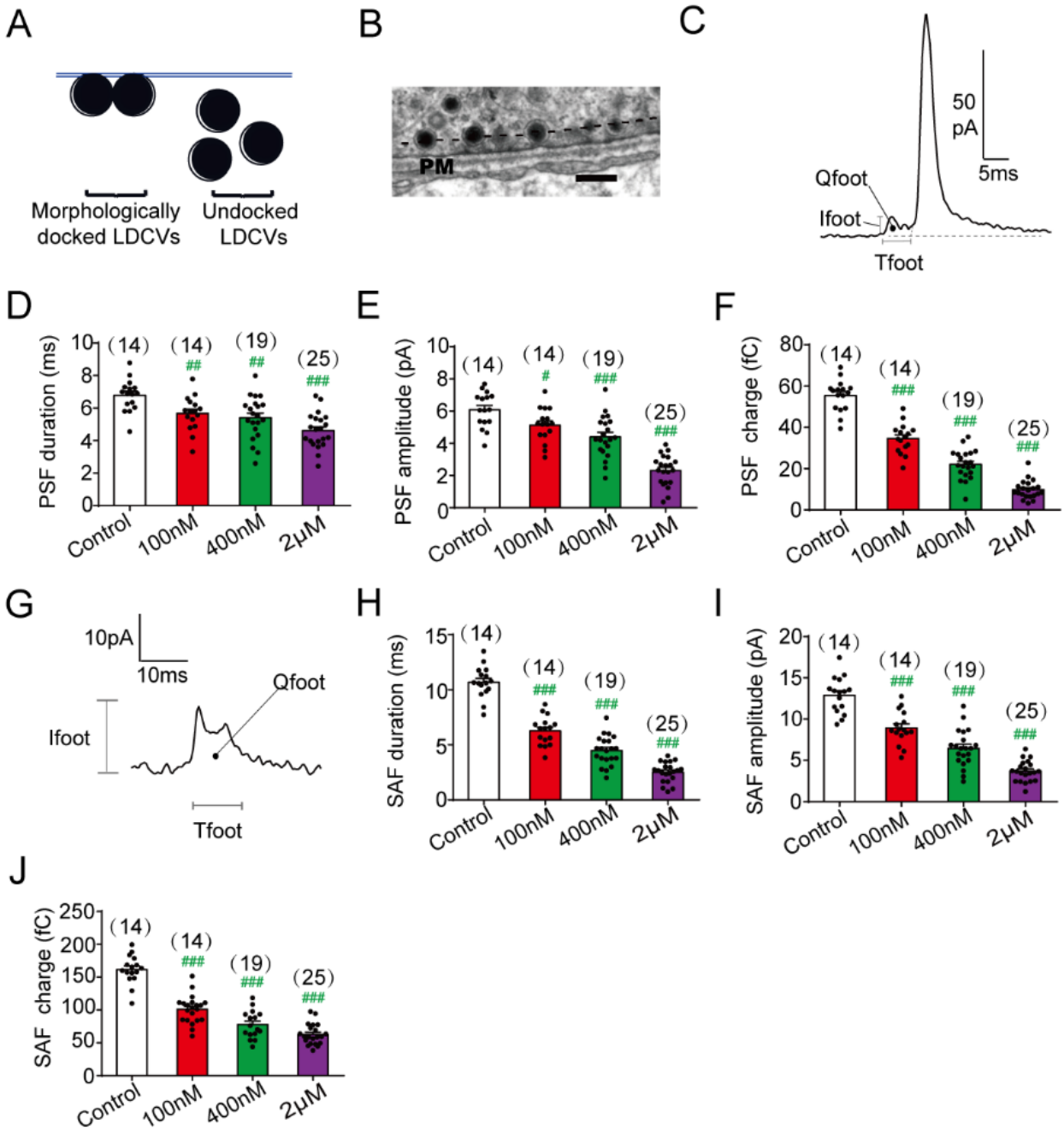

Appendix Figure S2. Effects of PTP-MEG2 inhibitor on the docking vesicles and PSF/SAF.

(A). Schematic image of the manifestations of morphological docking and undocked large dense core vesicles (LDCV).

(B). Representative image of morphological docking vesicles. Vesicles with distance less than 50nm (dashed line) from plasma membrane were defined as morphological docking vesicles. Scale bars: 150 nm.

(C). Representation of the pre-spike foot (PSF) by a typical spike in our electrochemical experiments. T_{foot} indicated the duration of the PSF, the I_{foot} indicated the amplitude of the PSF and the Qfoot indicated the total charge of the PSF.

(D-F). Different parameters of pre-spike foot of cells incubated with different dose of PTP-MEG2 inhibitor including the PSF duration (T_{foot}) (D), PSF amplititude (I_{foot}) (E), and PSF charge (Q_{foot}) (F) detected with electrochemical experiments were calculated from 72 chromaffin cells.

(G). Representation of the stand alone foot (SAF) in our electrochemical experiments. T_{foot} indicated the duration of the SAF, the I_{foot} indicated the amplitude of the SAF and the Qfoot indicated the total charge of the SAF.

(H-J). Different parameters of stand alone foot (SAF) of cells incubated with different dose of PTP-MEG2 inhibitor detected with electrochemical experiments were calculated, including SAF duration (T_{foot}) (H), SAF amplitude (I_{foot}) (I), and the average total charge (Q_{foot}) of SAF (J). Data information: # indicates the PTP-MEG2 inhibitor group compared with the control vehicle group. #, $P<0.05$; ##, $P<0.01$; ### $P<0.001$; N.S. means no significant difference. The bars represent mean ± s.e.m. (D-F), (H-J) Data were from 8 independent experiments. All the data were analysed using one-way ANOVA.

Appendix Figure S3

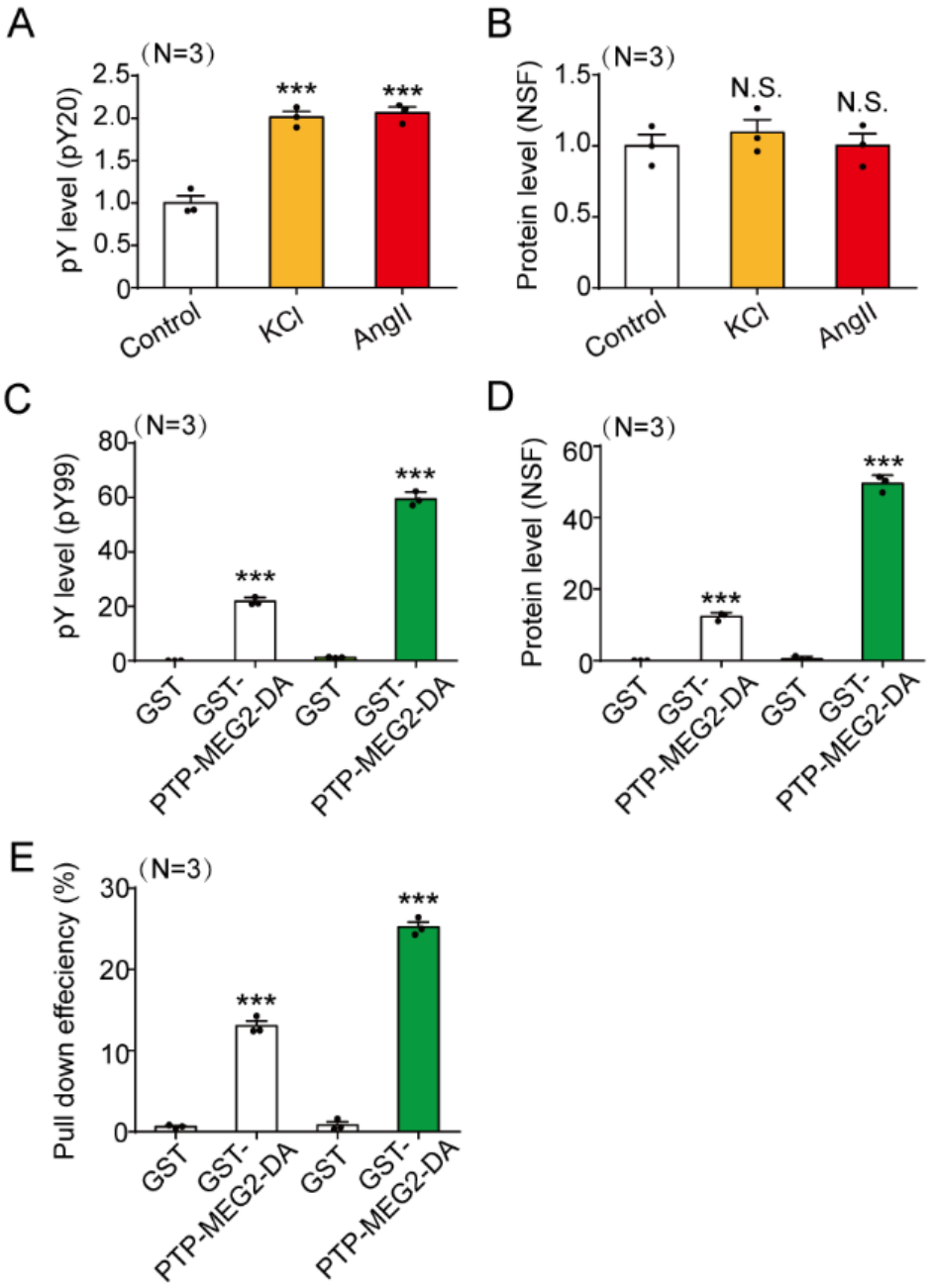

Appendix Figure S3. PTP-MEG2 interacts with and dephosphorylates tyrosine phosphorylated NSF in chromaffin cells.

(A-B). Tyrosine phosphorylation levels of the phosphorylated NSF (A) and total immunoprecipitated NSF (B) in Figure 2A detected with western blot were quantified. Data were normalized to the unstimulated control group.

(C-D). The protein expression levels of pY^{99} (C) and NSF (D) pulled down in Figure 2D detected with western blot were quantified. Data were normalized to GST control group.

(E) The pull-down efficiency of GST-MEG2-D^{470}A on NSF in Figure 2D was calculated by NSF (amount of output)/ NSF (amount of input)*100%.

Data information: *** represented $P<0.001$ compared with control group. N.S. means no significant difference. The bars represent mean ± s.e.m. The replicates number (N) is indicated in the graphs and refers to independent experiments in all panels. All the data were analysed using one-way ANOVA.

Appendix Figure S4

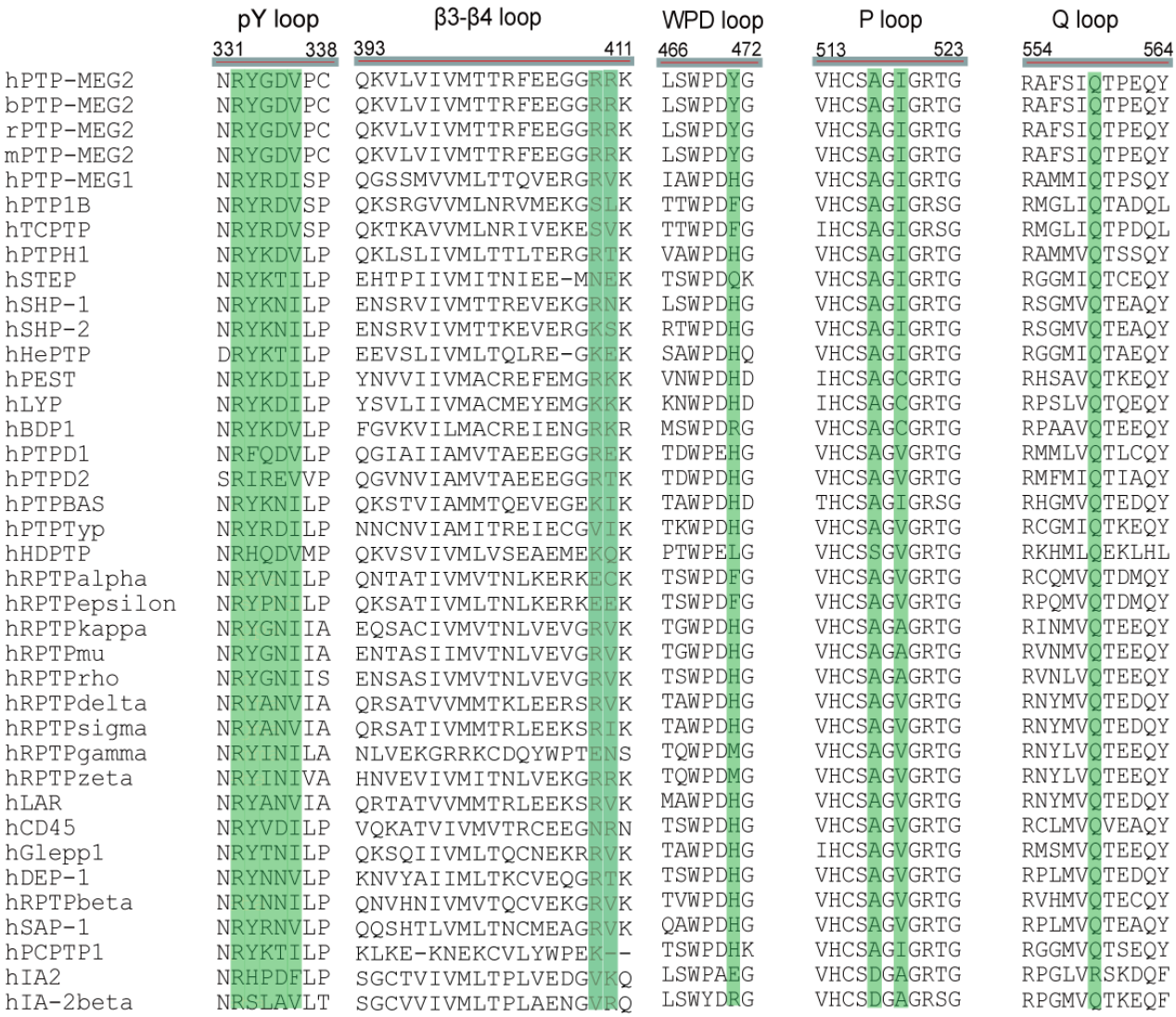

Appendix Figure S4. Sequence alignment of the PTP-MEG2.

The sequence alignment of the pY loop, β3-β4 loop, WPD loop, P loop, Q loop from different PTPs. Key residues involved in the interactions between PTP-MEG2 and NSF, as well as the PTP-MEG2 and MUNC18-1 are highlighted and compared with other PTP members.

Appendix Figure S5

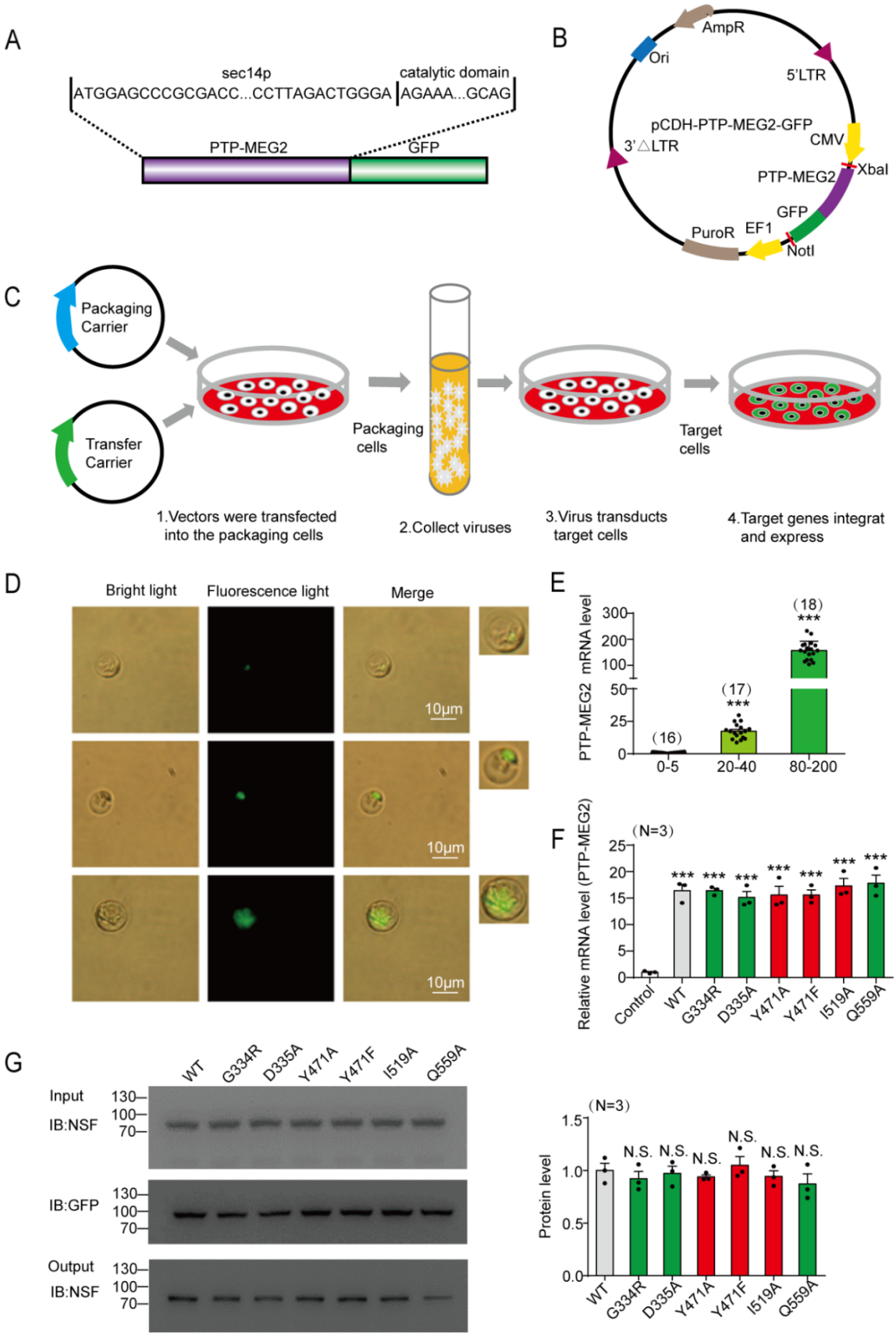

Appendix Figure S5. Effect of PTP-MEG2 mutations on catecholamine secretion from primary chromaffin cells.

(A).The nucleotide sequence of the PTP-MEG2-GFP construct used for overexpressing PTP-MEG2 in primary mouse chromaffin cells.

(B). Schematic diagram of PTP-MEG2-GFP lentivirus vector.

(C).Schematic representation of lentivirus containing PTP-MEG2 wild type or mutants production, transduction and expression in mouse primary chromaffin cells.

(D). Primary mouse chromaffin cells were transduced with lentivirus containing empty vector, wild-type PTP-MEG2, or different mutants with a GFP tag at the C-terminus. The fluorescence was excited at 488 nm and emission was recorded at 530 nm at same condition (Exposure time: 100ms. Resolution: 1920*1080).

(E). The bar graphs shows the relationship between quantified fluorescence intensity levels and mRNA levels of primary chromaffin cells transduced with lentivirus encoding PTP-MEG2 wild type. For mRNA quantification, the endogenous mRNA level of PTP-MEG2 was used as reference and the relative level of overexpressed PTP-MEG2 were represented as bar graph. For X-axis parameters, the intensity of fluorescence was quantified by Image J and calculated as (fluorescence brightness×fluorescence area). The relative fluorescence value was set up to 1 using purified GFP protein with a concentration of 10ng/ml and the intensities of other cells were quantified by ratio to this control. Cells with similar fluorescence intensity (0-5, 20-40 or 80-200) were subjected to mRNA extraction and qRT-PCR analysis targeting PTP-MEG2.

(F). After virus infection, the selected cells with fluorescence values between 20 and 40 in Appendix Figure S5 (D)-(E) were selected for mRNA quantification analysis. The bar graphs shows the quantified mRNA levels for each different PTP-MEG2 mutants.

(G). PC12 cells were infected with lentiviruses encoding PTP-MEG2-D^{470}A-GFP of wild type and different mutants. The GFP-affinity-beads were used in co-IP assay to examine the binding of PTP-MEG2 to endogenous NSF from PC12 cells. The bar graphs show the quantified NSF protein levels binding to different PTP-MEG2.

Data information: * in (E) indicates the difference of MEG2 mRNA levels in infected cells. * in (F) indicates the transduced PTP-MEG2 group compared with the empty vector group. ***, $P< 0.001$ compared with the control groups. N.S. represented no difference compared with the control groups. The bars represent mean ± s.e.m. (E) Data were from 6 independent experiments. The replicates number (N) is indicated in the graphs and refers to independent experiments in all panels. All the data were analysed using one-way ANOVA.

Appendix Figure S6

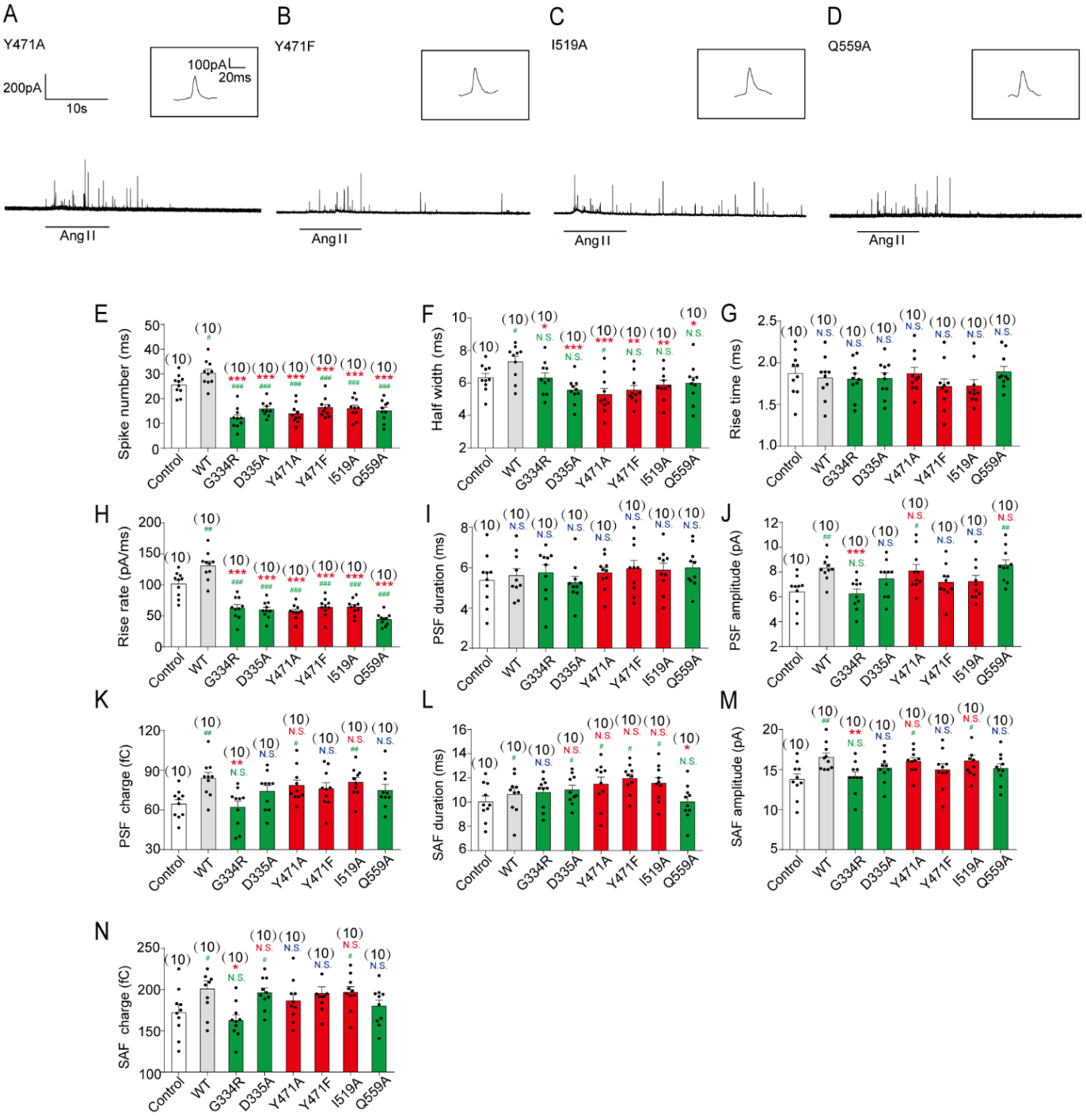

Appendix Figure S6. Effects of PTP-MEG2 mutations on catecholamine secretion from primary chromaffin cells.

(A-D). Representative image of amperometric spikes of primary mouse chromaffin cells overexpressing PTP-MEG2-Y^{471}A (A), PTP-MEG2-Y^{471}F (B), PTP-MEG2-I^{519}A (C) and PTP-MEG2-Q^{559}A (D) in response to 100nM AngII stimulation detected with electrochemical experiments .

(E-N). Quantitative analysis of the amperometric spikes of primary mouse chromaffin cells transduced with different PTP-MEG2 mutations in PTP-MEG2-phospho-NSF-pY^{83} segment interface detected with electrochemical experiments. Parameters of amperometric spikes included spike number (E), half width (F), rise time (G), rise rate (H), PSF duration (I), PSF amplitude (J), PSF charge (K), SAF duration (L), SAF amplitude (M) and SAF charge (N).

Data information: * indicates PTP-MEG2 mutants overexpression groups compared with the WT overexpression group. # indicates the overexpression group compared with the control group. *, $P<0.05$; **, $P<0.01$; *** $P<0.001$ and #, $P<0.05$; ##, $P<0.01$; ### $P<0.001$. N.S. represented no difference compared with the control groups. The bars represent mean ± s.e.m. Data were from 6 independent experiments. All the data were analysed using one-way ANOVA.

Appendix Figure S7

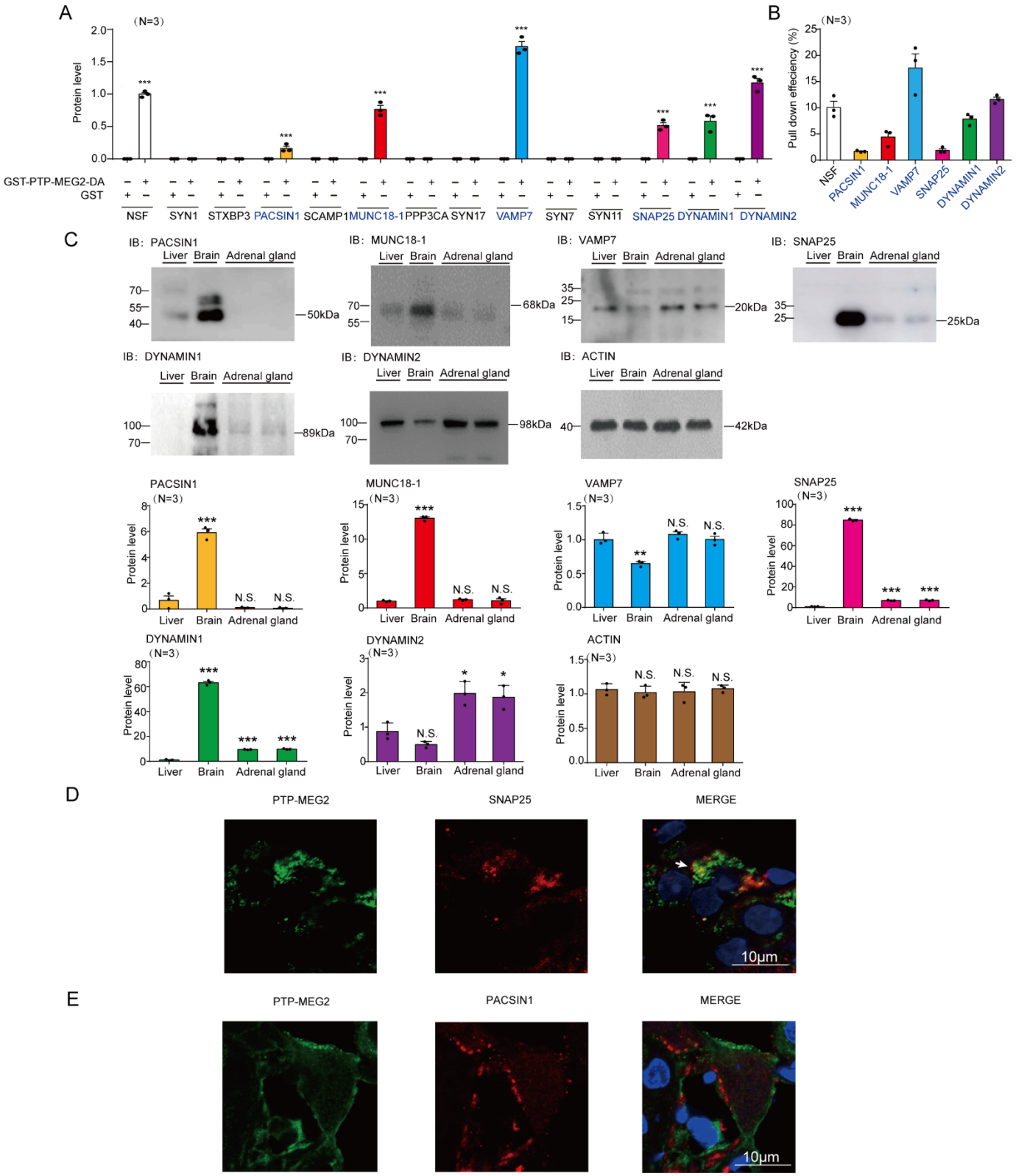

Appendix Figure S7. Screening and identification of candidate PTP-MEG2 substrates involved in PSF/SAF regulation.

(A). Protein levels of the pull down assay in Figure 6C were quantified. * represented GST-PTP-MEG2-$D^{470}A$ group compared with corresponding control GST group.

(B). The pull-down efficiency of GST-MEG2-$D^{470}A$ in Figure 6C on NSF, PACSIN1, MUNC18-1, VAMP7, SNAP25, DYNAMIN1, and DYNAMIN2 was calculated with (protein amount of output)/ (protein amount of input)*100%.

(C). Upper panel: the expression of PACSIN1, MUNC18-1, VAMP7, SNAP25, DYNAMIN1, and DYNAMIN2 in mouse liver, brain and adrenal gland was detected with western blot using specific antibodies. Bottom panel: qualification of PACSIN1, MUNC18-1, VAMP7, SNAP25, DYNAMIN1 and DYNAMIN2 protein levels in different tissues. * indicates the other tissues compared with liver.

(D-E). Co-localization of PTP-MEG2, SNAP25 (D), and PACSIN1 (E) in adrenal gland medulla was detected with immunofluorescence. White arrow stands for significant co-localization of PTP-MEG2, SNAP25, and PACSIN1. Rat adrenal medulla was incubated in 100 nM AngII for 1 minutes and fixed with formalin and sliced into 4-μm slides. Primary antibodies of PTP-MEG2 or candidate proteins (SNAP25, PACSIN1) were used to incubated with the slides overnight at 4℃. Secondary antibodies labeled with FITC (green) or TRITC (red) were applied for 1 hour at 25℃. Images were captured with confocal microscope.

Data information: *, $P<0.05$; **, $P<0.01$; *** $P<0.001$. N.S. represented no difference compared with the control groups. The bars represent mean ± s.e.m. The replicates number (N) is indicated in the graphs and refers to independent experiments in all panels. All the data were analysed using one-way ANOVA.

Appendix Figure S8

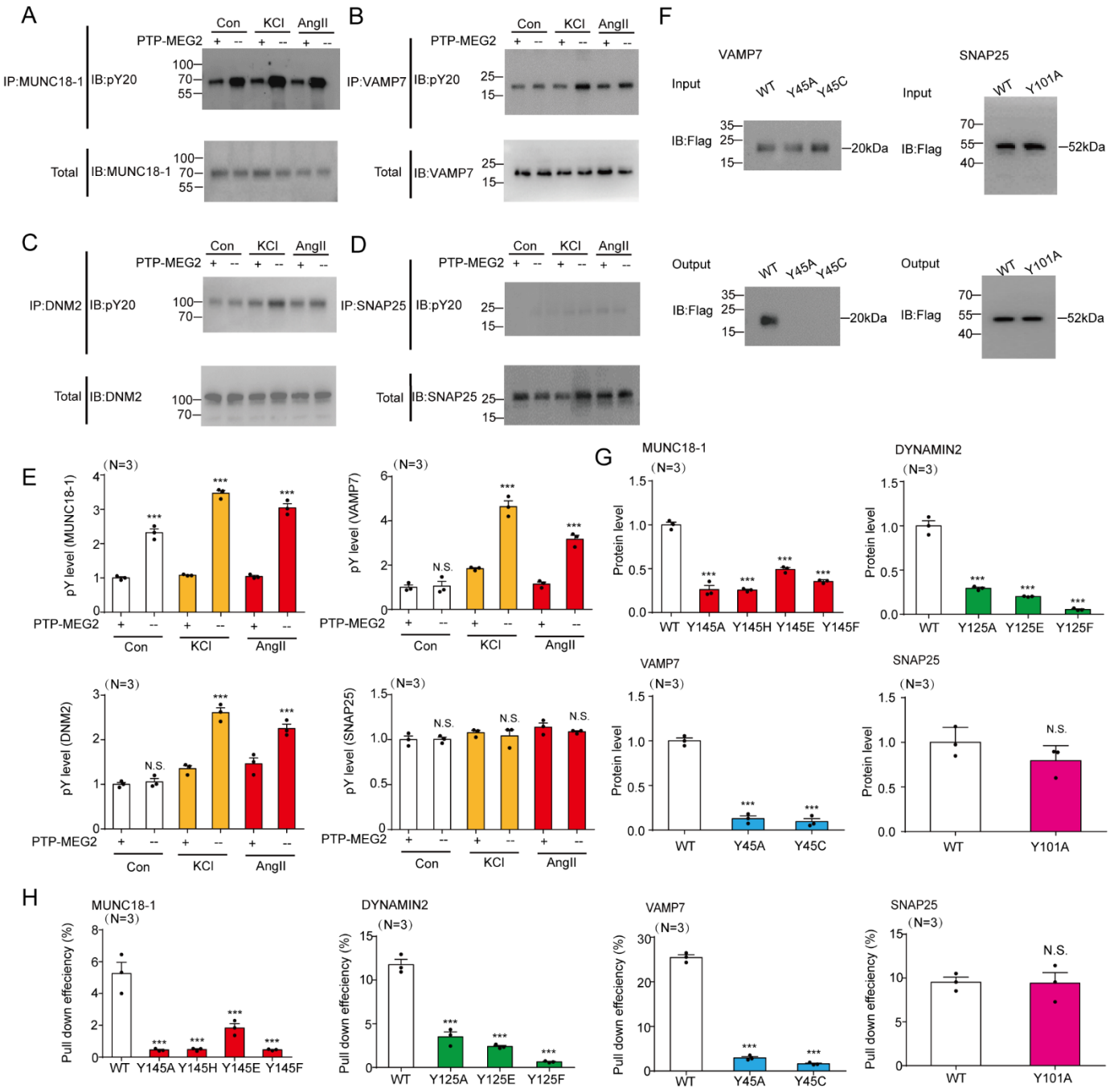

Appendix Figure S8. Influence of PTP-MEG2 on the phosphorylation of MUNC18-1, VAMP7, DYNAMIN2 and SNAP25.

(A-D). Tyrosine phosphorylation levels of MUNC18-1 (A), VAMP7 (B), DYNAMIN2 (C), and SNAP25 (D) in primary rat chromaffin cells were monitored. Rat adrenal medulla was lysed and incubated with Protein A/G beads after stimulation with 100nM AngII for 5 minutes, in presence or absence of 5μg PTP-MEG2 catalytic domain protein. Protein A/G beads were pre-incubated with primary antibody of MUNC18-1, VAMP7, DYNAMIN2, or SNAP25. Pan-phosphorylation antibody pY^{20} was used to detect the phosphorylation of proteins binding with the complex of antibody-Protein A/G beads.

(E). The quantification of the tyrosine phosphorylation levels of MUNC18-1, VAMP7, DYNAMIN2, and SNAP25 recognized by pY^{20} antibody.

(F). Interactions of the PTP-MEG2-trapping mutants with the VAMP7-Y^{45}A or Y^{45}C mutants (left), SNAP25-Y^{101}A (right). PC12 cells were transfected with the FLAG-tagged VAMP7 wild type or Y^{45}A or Y^{45}C mutants; FLAG-GFP-tagged SNAP25 wild type or Y^{101}A mutant 24 hours before stimulation with 100 nM AngII respectively. The cell lysates were then incubated with the GST beads-PTP-MEG2-D^{470}A protein for 2 hours under constant rotation. The potential PTP-MEG2 substrates were pulled down by GST-beads and their levels were examined by the FLAG antibody with western blot.

(G). Protein levels in Figure 7 (D) and Appendix Figure S8 (F) were quantified.

(H). The pull-down efficiency of GST-MEG2-D^{470}A in Figure 7(D) and Appendix Figure S8 (F) on MUNC18-1 wide type and mutations, DYNAMIN2 wide type and mutations, VAMP7 wide type and mutations, SNAP25 wide type and mutations, were calculated with (protein amount of output)/(protein amount of input)*100%.

Data information: *** represented $P<0.001$ and N.S. represented no difference compared with corresponding control group. The bars represent mean ± s.e.m. The replicates number (N) is indicated in the graphs and refers to independent experiments in all panels. All the data were analysed using one-way ANOVA.

Appendix Figure S9

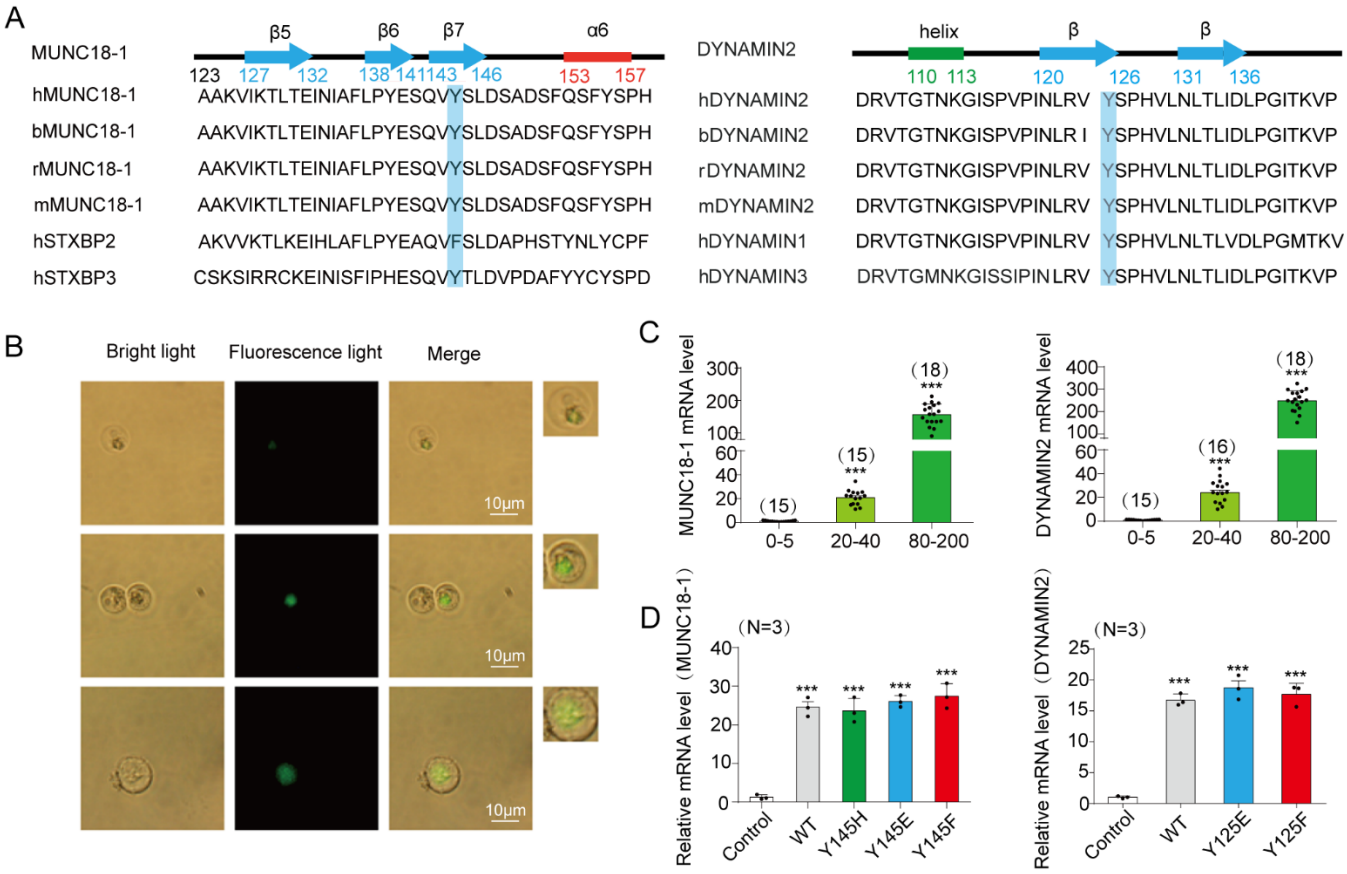

Appendix Figure S9. MUNC18-1-Y^{145} and DYNAMIN2-Y^{125} are essential in PTP-MEG2 regulation of PSF/SAF.

(A). Sequence alignment of amino acids surrounding MUNC18-1-Y^{145} and DYNAMIN2-Y^{125}. The MUNC18-1-Y^{145} and DYNAMIN2-Y^{125} sites were highlighted with blue.

(B).Primary mouse chromaffin cells were infected with lentivirus containing control vector, wild-type MUNC18-1, DYNAMIN2, or different mutants of these two proteins. The fluorescence was excited at 488 nm and emission was recorded at 530 nm at same condition (Exposure time: 100ms. Resolution: 1920*1080).

(C). The bar graphs shows the relationship between quantified fluorescence intensity levels and mRNA levels of MUNC18-1 and DYNAMIN2. The mRNA level of endogenous MUNC18-1 and DYNAMIN2 in primary chromaffin cells were used as reference to quantify the overexpressed MUNC18-1 and DYNAMIN2, respectively. The fluorescence intensity was analyzed with Image J and calculated as (fluorescence brightness×fluorescence area). For X-axis parameters, the intensity of fluorescence was quantified by Image J. The relative fluorescence value was set up to 1 using purified GFP protein with a concentration of 10ng/ml and the intensities of other cells were quantified by ratio to this control. Cells with similar fluorescence intensity (0-5, 20-40 or 80-200) were subjected to mRNA extraction and qRT-PCR analysis targeting MUNC18-1 or DYNAMIN2.

(D). After virus infection, cells with fluorescence values between 20 and 40 in Appendix Figure S9 (B)-(C) were selected for mRNA extraction and qRT-PCR analysis. The bar graphs show the quantified mRNA levels for wide-type or each different MUNC18-1 (left panel) or DYNAMIN2 (right panel) mutants. The mRNA data were normalized to endogenous MUNC18-1 or DYNAMIN2 mRNA level in control vector-infected cells.

Data information: * in (C) indicates the difference of MUNC18-1 or DYNAMIN2 mRNA levels in infected cells. * in (D) indicates the transduced MUNC18-1 or DYNAMIN2 group compared with the empty vector group. *** represents $P<0.001$ compared with the control groups. The bars represent mean ± s.e.m. (C) Data were from 6 independent experiments. The replicates number (N) is indicated in the graphs and refers to independent experiments in all panels. All the data were analyzed using one-way ANOVA.

Appendix Figure S10

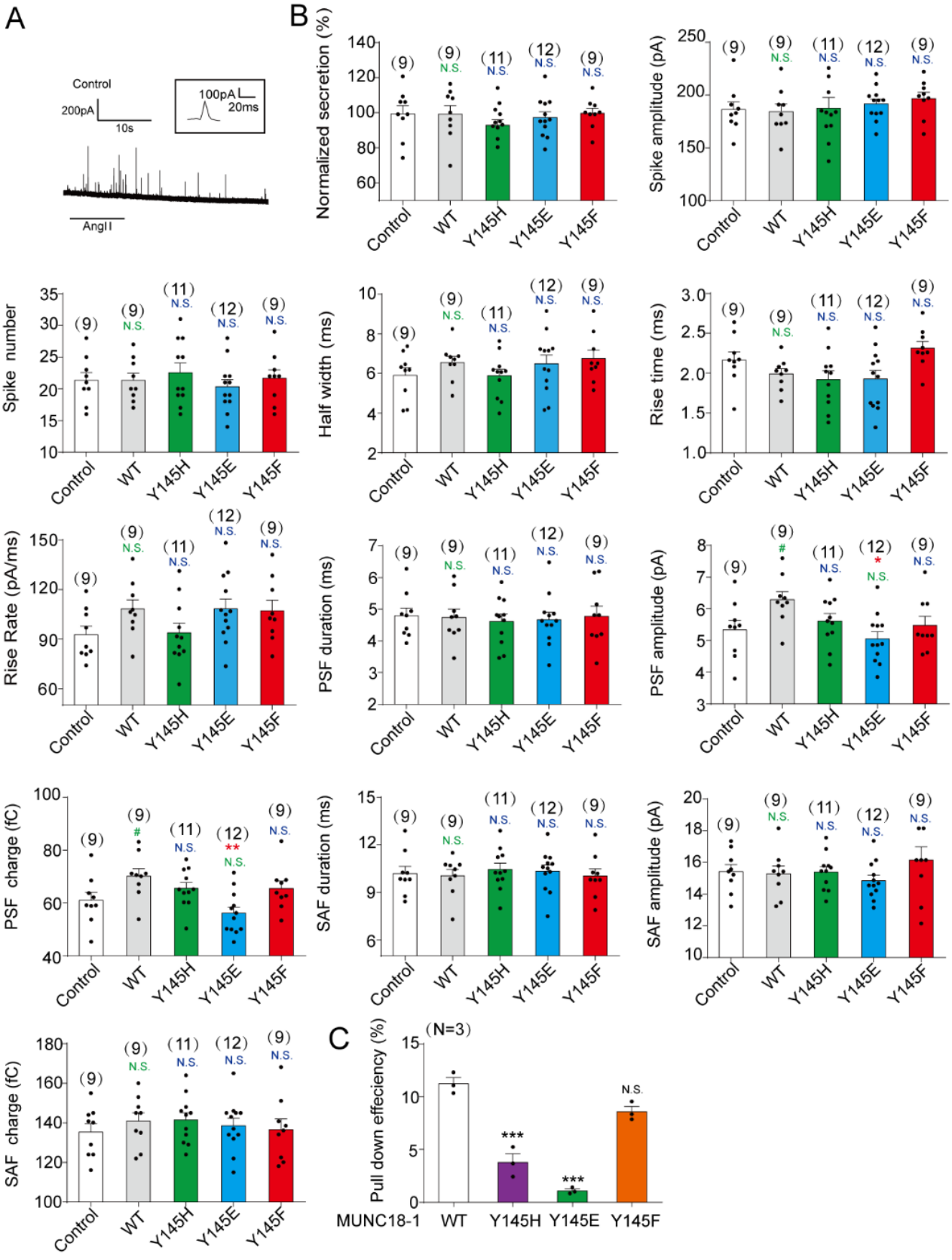

Appendix Figure S10. MUNC18-1-Y^{145} is essential in PTP-MEG2 regulation of PSF/SAF.

(A). Primary chromaffin cells were transduced with lentivirus containing empty vector. These cells were stimulated with 100nM AngII. The amperometric spikes were detected with electrochemical experiments. Typical amperometric traces are shown.

(B). Parameters of amperometric spikes of primary chromaffin cells overexpressing empty vector ， MUNC18-1 wild type, MUNC18-1-Y^{145}H, Y^{145}E or Y^{145}F mutants were detected with electrochemical experiments. Primary chromaffin cells were transfected with empty vector, MUNC18-1-WT, Y^{145}H, Y^{145}E, or Y^{145}F by lentivirus and stimulated with AngII (100nM). The amperometric spikes including the secretion amount, spike amplitude, spike number, half width, rise time, rise rate, parameters of PSF and SAF were compared among empty vector, wild type, and mutations.

(C). Pull down efficiency of SYNTAXIN1 in Figure 7H was evaluated by calculating with (protein amount of output)/(protein amount of input)*100%..

Data information: * indicates MUNC18-1 mutants overexpression groups compared with the WT overexpression group. # indicates MUNC18-1 overexpression group compared with the control group. *, $P<0.05$; **, $P<0.01$; ***, $P<0.001$ and #, $P<0.05$. N.S. represented no difference compared with corresponding control group. The bars represent mean ± s.e.m. Data were from 6 independent experiments. All the data were analysed using one-way ANOVA.

Appendix Figure S11

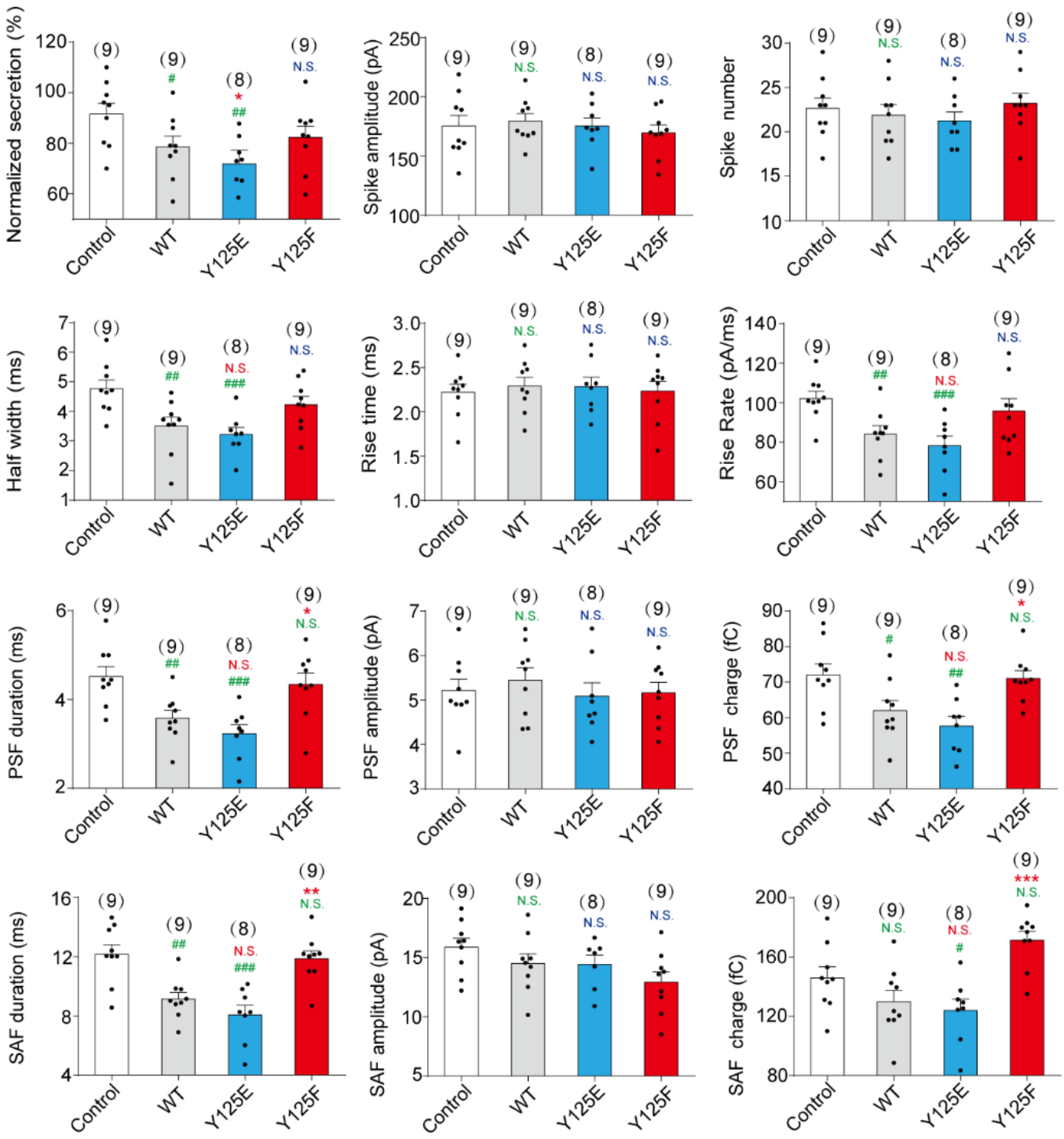

Appendix Figure S11. DYNAMIN2-Y^{125} is essential in PTP-MEG2 regulation of PSF/SAF.

Parameters of amperometric spikes of primary chromaffin cells overexpressing empty vector, DYNAMIN2 wild type, DYNAMIN2-Y^{125}E or Y^{125}F mutants were detected with electrochemical experiments. Primary chromaffin cells were transducted with empty vector, DYNAMIN2-WT, Y^{125}E, or Y^{125}F by lentivirus and stimulated with AngII (100nM). The amperometric spikes including the secretion amount, spike amplitude, spike number, half width, rise time, rise rate, parameters of PSF and SAF were compared among empty vector, wild type, and mutants. Data information: * indicates DYNAMIN2 mutants overexpression compared with the WT overexpression group. # indicates DYNAMIN2 overexpression group compared with the control group. *, $P<0.05$; **, $P<0.01$; ***, $P<0.001$ and #, $P<0.05$; ##, $P<0.01$; ###, $P<0.001$. N.S. represented no difference compared with corresponding control group. The bars represent mean ± s.e.m. Data were from 6 independent experiments. All the data were analysed using one-way ANOVA.

Appendix Figure S12

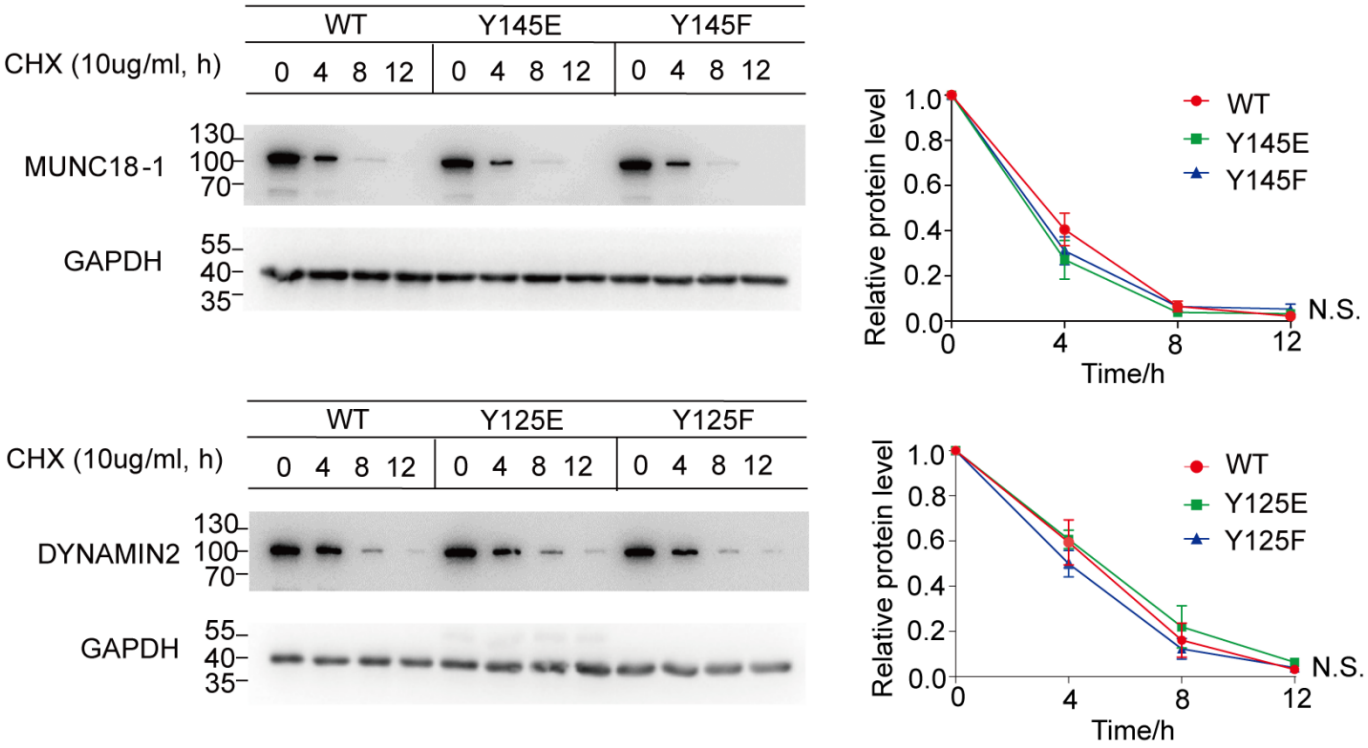

Appendix Figure S12. Mutations of MUNC18-1/DYNAMIN2 had no influence on the degradation.

HEK293 cells were seeded in 6-well plates. Cells were transfected with plasmids encoding MUNC18-1/DYNAMIN2 WT or different mutants for 24 h. Then they were treated with cycloheximide (CHX) and harvested at different time points (0, 4, 8, 12h) for western blot analysis. The band intensity of MUNC18-1 or DYNAMIN2 was quantified (right panel). Data were obtained from 3 independent experiments and displayed with mean ± s.e.m. N.S. represented no difference compared with control group. All statistical significance was calculated with one-way ANOVA.

Appendix Figure S13

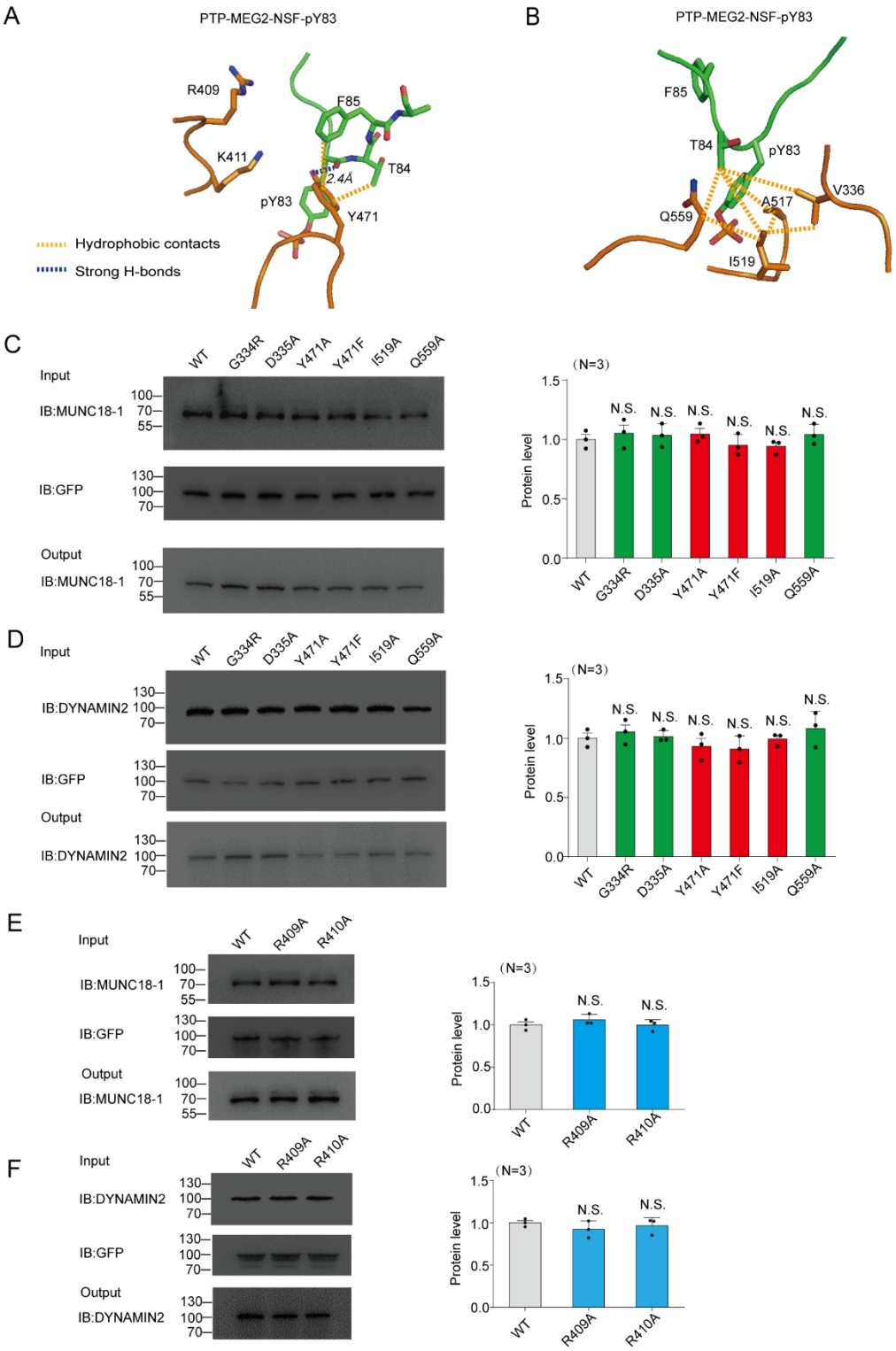

Appendix Figure S13. The structural comparison of PTP-MEG2 in complex with phospho-segment derived from different substrates and interaction of PTP-MEG2-WT and different mutants toward MUNC18-1 and DYNAMIN2.

(A-B). The detailed interactions of the PTP-MEG2 Y^{471} (A) or I^{519} (B) and the NSF-pY^{83} phospho-segment.

(C-F). PC12 cells were infected with lentiviruses encoding PTP-MEG2-D^{470}A-GFP of wild type and different mutants. Co-IP assays to were used to examine the binding of different PTP-MEG2 mutants to endogenous MUNC18-1 (C, E) and DYNAMIN2 (D, F), using the GFP-beads.

Data information: N.S. represented no difference compared with corresponding WT group. The bars represent mean ± s.e.m. The replicates number (N) is indicated in the graphs and refers to independent experiments in all panels. All the data were analyzed using one-way ANOVA.

Appendix Figure S14

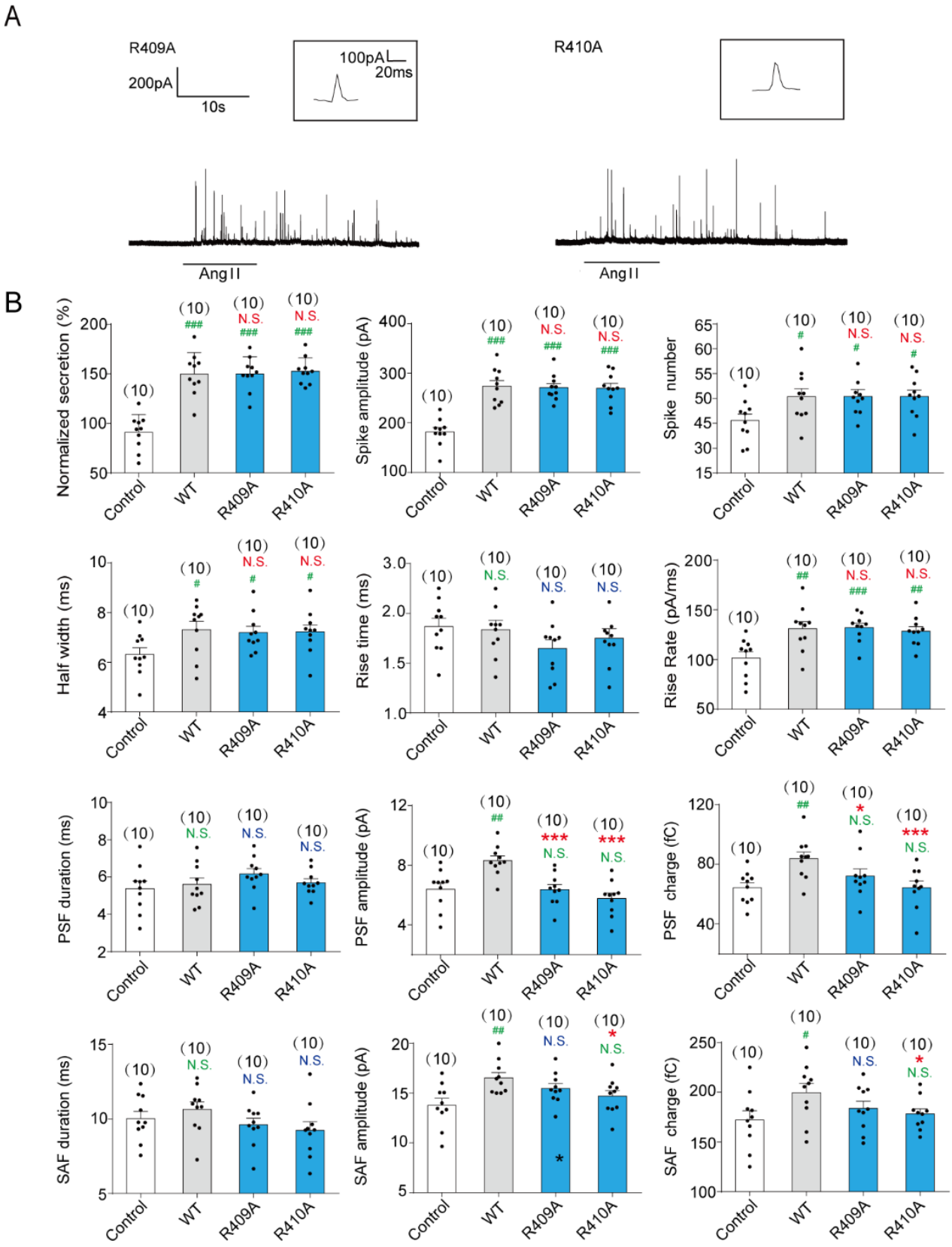

Appendix Figure S14. Effect of PTP-MEG2-R^{409}A or R^{410}A mutations on catecholamine secretion from primary chromaffin cells.

(A). Primary chromaffin cells were transduced with lentivirus containing PTP-MEG2-R^{409}A/R^{410}A. These cells were stimulated with 100nM AngII. The amperometric spikes were detected with electrochemical experiments. Typical amperometric traces are shown.

(B). Parameters of amperometric spikes of primary chromaffin cells overexpressing PTP-MEG2-R^{409}A or R^{410}A mutants detected with electrochemical experiments. Primary chromaffin cells were transfected with PTP-MEG2-R^{409}A or R^{410}A mutants by lentivirus and stimulated with AngII (100nM). The amperometric spikes including the secretion amount, spike amplitude, spike number, half width, rise time, rise rate, parameters of PSF and SAF were compared between empty vector, wild type, and mutation.

Data information: * indicates PTP-MEG2-R^{409}A or R^{410}A mutants overexpression groups compared with the WT overexpression group. # indicates PTP-MEG2 overexpression group compared with the control group. *, $P<0.05$; ***, $P<0.001$ and #, $P<0.05$; ##, $P<0.01$; ### $P<0.001$. N.S. represented no difference compared with corresponding control group. The bars represent mean ± s.e.m. Data were from 6 independent experiments. All the data were analysed using one-way ANOVA.

Appendix Table S1. Catalytic activity of PTP-MEG2-WT and different mutants toward pNPP and pY^{83}-NSF.

pNPP

Enzymes	k_{cat} [s^{-1}]	Km [mM]	k_{cat}/K_m [10^3, $M^{-1}\cdot s^{-1}$]	Fold of Activity Decrease
WT	6.65±0.13	10.90±0.40	0.61±0.01	1.00
Y333A	1.39±0.05	23.30±1.00	0.06±0.01	10.14
G334R	4.76±0.24	6.90±1.00	0.69±0.07	0.88
D335A	3.47±0.28	5.10±0.60	0.68±0.03	0.89
Y471A	1.43±0.04	2.60±0.70	0.55±0.13	1.11
Y471F	2.70±0.05	5.40±0.60	0.50±0.05	1.21
I519A	2.55±0.03	15.00±0.80	0.17±0.01	3.53
Q559A	0.49±0.01	1.10±0.10	0.45±0.03	1.35

NSF

Enzymes	k_{cat}/K_m [10^5, $M^{-1}\cdot s^{-1}$]	Fold of Activity Decrease	Selectivity for Peptide
WT	85.20±2.50	1.00	1.00
Y333A	0.20±0.03	436.79	43.00
G334R	14.10±1.50	6.04	6.86
D335A	8.15±0.14	10.45	11.74
Y471A	5.59±0.17	15.24	13.73
Y471F	3.69±0.12	23.09	19.08
I519A	0.15±0.01	550.32	155.89
Q559A	0.04±0.01	2027.40	1501.80

Appendix Table S2. Candidate proteins were selected by Pubtator or STRING

name	source	methods	gene_id	PMID
MAPK1	STRING	Coexpression Experiments textmining	5594	9892209
PHLPP1	STRING	Coexpression Experiments textmining	23239	20733099
RET	Pubtator	textmining	373625/5979	10484767
SEC14L1	STRING	textmining	6397	9670016
SRC	Pubtator	textmining	6714/20779	20530578 24582588 23333852 14963047 21097543 10523831
Syntaxin 17	Pubtator	textmining	420995	23006999
GRK5	Pubtator	textmining	2869	21097543
GELSOLIN	Pubtator	textmining	2934	10210201
Grb2	Pubtator	textmining	2885/14784	14963047 14576154 10995764 10995764 10523831
NSF	STRING/Pubtator	Coexpression Experiments textmining	4780	22679448
The dynamin-binding-protein actin	Pubtator	textmining	23268	28918902
Cell division cycle 42	Pubtator	textmining	998	8836113
DYNAMIN 2	Pubtator	textmining	13430/1785	25468568
Dyrk1A	Pubtator	textmining	1859/13548	22765017
INSR	STRING	Experiments textmining	408017	9448292
MAPK3	STRING	Coexpression Experiments textmining	102188824	9892209
SNAP-23	Pubtator	textmining	8773	21097543
STAT3	STRING	textmining	6774	9973406
MUNC18-3	Pubtator	textmining	6814	21548926
TI-VAMP/VAMP7	Pubtator	textmining	6845	23471971
AS160	Pubtator	textmining	9882	21454690
CEACAM8	Pubtator	textmining	1088	24926560 21097543
FcRy	Pubtator	textmining	127943	16263223
GLUT4	Pubtator	textmining	6517	21454690
mannose receptor	Pubtator	textmining	4360	28978467
MAPK15	STRING	Coexpression Experiments textmining	225689	9892209
MAPK4	STRING	Coexpression Experiments textmining	54268	9892209
maturation-promoting-factor	Pubtator	textmining	380246	22252323
p38	Pubtator	textmining	1432	14963047 24926560 14576154 21097543

PTP1B	Pubtator	textmining	5770	22045810
SCAMP 1	Pubtator	textmining	9522	9658162
MUNC18-1	Pubtator	textmining	25558	23962429
Cav1.1	Pubtator	textmining	779	15793008
Cav1.2	Pubtator	textmining	775	16554304
DYNAMIN 1	Pubtator	textmining	1759	12011079
Fgr	Pubtator	textmining	2268	21097543
Hck	Pubtator	textmining	3055	21097543
IGF-I	Pubtator	textmining	3479/16000	14963047 10847583
Lck	Pubtator	textmining	3932	27091106
Pacsin 1	Pubtator	textmining	29993	23420842
PHLPP2	STRING	textmining	23035	20031553
PTPRT	Pubtator	textmining	362263	23962429 23962429
SHP-1	Pubtator	textmining	8431	24216759 10995764
SNAP 25	Pubtator	textmining	6616	30267828
Synapsin 1	Pubtator	textmining	6853	20530578
Synaptotagmin 1	Pubtator	textmining	6857	29414700
v-SNARE	Pubtator	textmining	10490	23471971
Synaptotagmin 7	Pubtator	textmining	9066	29088700
Synaptotagmin 11	Pubtator	textmining	23208	28686317
PPP3ca	Pubtator	textmining	5530	24835995
PTC3	Pubtator	textmining	734285	7624118

Appendix Table S3. The expression of 28 candidate genes in adrenal gland.

gene_name	Tissue atlas
PHLPP1	high
SRC	high
NSF	low
GRK5	low
INSR	medium
Cell division cycle 42	medium
SNAP-23	medium
TI-VAMP/VAMP7	medium
CEACAM8	not detected
GLUT4	low
mannose receptor	N.A.
MUNC18-1	N.A.
DYNAMIN 2	medium
MUNC18-3	medium
Cav1.1	medium
Cav1.2	medium
DYNAMIN 1	low
Fgr	not detected
Hck	not detected
Lck	not detected
PACSIN 1	low
PTPRT	not detected
SNAP 25	high
Synapsin 1	low
v-SNARE	medium
protein phosphatase 3 catalytic subunit alpha	medium
Synaptotagmin 7	medium
Synaptotagmin 11	low

Appendix Table S4. The peptide information in LC-MS/MS.

b^+	Sequence	y^+	y^{2+}
	V		
343.11	p-Y		1037.55
430.14	S		916.04
	P		
664.25	H		
763.32	V		
876.40	L	1410.86	
990.44	N		
1103.82	L		
1204.88	T	1070.65	
1317.66	L	969.60	
1430.74	I	856.51	
1545.77	D	743.43	
1658.85	L	628.40	
	P	515.38	258.16
	G	418.27	
	I	361.24	
	T	248.16	
	K	147.11	

Appendix Table S5. Catalytic activity of PTP-MEG2-WT and different mutants toward pY^{145}-MUNC18-1 and pY^{125}-DYNAMIN2.

MUNC18-1

Enzymes	k_{cat}/K_m [10^5, $M^{-1}\cdot s^{-1}$]	Fold of Activity Decrease	Selectivity for Peptide
WT	146.00±12.00	1.00	1.00
Y333A	6.81±0.25	21.60	2.12
G334R	18.90±1.60	7.75	8.81
D335A	3.19±0.20	46.00	51.28
R409A	27.55±0.62	5.33	6.56
R410A	10.97±0.47	13.39	5.70
Y471A	108.00±4.60	1.35	1.21
Y471F	115.00±4.70	1.28	1.05
I519A	187.00±14.00	0.78	0.22
Q559A	17.50±0.67	8.41	6.21

DYNAMIN2

Enzymes	k_{cat}/K_m [10^5, $M^{-1}\cdot s^{-1}$]	Fold of Activity Decrease	Selectivity for Peptide
WT	106.00±8.30	1.00	1.00
Y333A	23.40±1.25	4.54	0.45
G334R	24.80±1.20	4.29	4.88
D335A	7.02±0.30	15.20	16.90
R409A	24.12±0.57	4.41	5.43
R410A	9.98±0.62	10.67	4.55
Y471A	97.90±3.30	1.08	0.98
Y471F	61.90±2.70	1.72	1.41
I519A	31.90±4.20	3.33	0.93
Q559A	8.93±0.32	11.90	8.78

Appendix Table S6. REAGENT or RESOURCE

REAGENT or RESOURCE	SOURCE	IDENTIFIER
Antibodies		
NSF Antibody	Proteintech	Cat # 21172-1-AP
NSF Antibody	Santa Cruz	Cat # sc-515043
MUNC18-1 Antibody	Proteintech	Cat # 11459-1-AP
MUNC18-1 Antibody	Proteintech	Cat # 67137-1-lg
VAMP7 Antibody	Proteintech	Cat # 22268-1-AP
VAMP7 Antibody	Santa Cruz	Cat # sc-166394
SNAP25 Antibody	Proteintech	Cat # 60159-1-lg
SNAP25 Antibody	Proteintech	Cat # 14903-1-AP
PACSIN1 Antibody	Proteintech	Cat # 13219-1-AP
SYNTAXIN1a Antibody	Proteintech	Cat # 66437-1-lg
pTyr(PY20) Antibody	Santa Cruz	Cat # sc-508
pTyr(PY99) Antibody	Santa Cruz	Cat # sc-7020
FLAG Antibody	Cell Signaling Technology	Cat # 2368
GAPDH Antibody	Cell Signaling Technology	Cat # 5174
PTP-MEG2 Antibody	R&D Systems	Cat # MAB2668
DYNAMIN1 Antibody	Abcam	Cat # AB52611
DYNAMIN2 Antibody	Abcam	Cat # AB65556
DYNAMIN2 Antibody	Santa Cruz	Cat # sc-166669
Chemicals, Peptides, and Recombinant Proteins		
Anti-GST-tag beads	TransGen Biotech Co., Ltd	Cat # DP201
Anti-GFP-tag beads	AlpaLife by KangTi Co., Ltd.	Cat # KTSM1301
Protein A/G-PLUS-Agarose	Santa Cruz	Cat # sc-2003
Ni-NTA Agarose	Thermo Fisher scientific	Cat # R90101
he phospho-peptide of NSF “EVSLpYTFDK”	China Peptides Co., Ltd	N/A

The phospho-peptide of MUNC18-1 “ESQVpYSLDS”	China Peptides Co., Ltd	N/A
The phospho-peptide of DYNAMIN2 “NLRVpYSPHV”	China Peptides Co., Ltd	N/A
Mouse EPI ELISA Kit	Shanghai Jianglai Co.,Ltd	JL11194-48T
Mouse NE ELISA Kit	Shanghai Jianglai Co.,Ltd	JL13969-96T
Angiotensin II (HDRVYIHPF-OH)	China Peptides Co., Ltd	N/A
Compound 7(PTP-MEG2 inhibitor)	Synthesized as previously described (Zhang et al., 2012)	
Experimental Models: Cell Lines		
293	ATCC	CRL-1573
293T	ATCC	CRL-3216
PC12	ATCC	CRL-1721
Software and Algorithms		
PyMol	Schrödinger	https://www.pymol.org/
CCP4i	Instruct Associate Centre for Integrated Structural Biology	http://www.ccp4.ac.uk/
Phenix	The PHENIX Industrial Consortium	https://www.phenix-online.org
Igor	Fourier Transform	https://www.wavemetrics.com/
Prism	GraphPad	http://www.graphpad.com

Appendix Table S7. Plasmid information

Plasmid	Vehicle information	Tag information
NSF	PCDNA3.1	FLAG
His-PTPMEG2-WT	pET-15b	His
His-PTPMEG2-333Y-A	pET-15b	His
His-PTPMEG2-334G-R	pET-15b	His
His-PTPMEG2-335D-A	pET-15b	His
His-PTPMEG2-471Y-A	pET-15b	His
His-PTPMEG2-471Y-F	pET-15b	His
His-PTPMEG2-519I-A	pET-15b	His
His-PTPMEG2-559Q-A	pET-15b	His
His-PTPMEG2-409R-A	pET-15b	His
His-PTPMEG2-410R-A	pET-15b	His
PCDH-PTPMEG2-WT	PCDH	GFP
PCDH-PTPMEG2-334G-R	PCDH	GFP
PCDH-PTPMEG2-335D-A	PCDH	GFP
PCDH-PTPMEG2-471Y-A	PCDH	GFP
PCDH-PTPMEG2-471Y-F	PCDH	GFP
PCDH-PTPMEG2-519I-A	PCDH	GFP
PCDH-PTPMEG2-559Q-A	PCDH	GFP
PCDH-PTPMEG2-409R-A	PCDH	GFP
PCDH-PTPMEG2-410R-A	PCDH	GFP
SYN1	PEGFP-N1	FLAG GFP
MUNC18-3	PEGFP-N1	FLAG GFP
PACSIN1	PEGFP-N1	FLAG GFP
SCAMP1	PEGFP-N1	FLAG GFP
MUNC18-1	PEGFP-N1	FLAG GFP
PPP3CA	PEGFP-N1	FLAG GFP
STX17	PEGFP-N1	FLAG GFP
VAMP7	CMV10	FLAG
SYT7	PEGFP-N1	FLAG GFP
SYT11	PEGFP-N1	FLAG GFP
SNAP25	PEGFP-N1	FLAG GFP
DYNAMIN1	CMV10	FLAG YFP
DYNAMIN2	pMYC-C2	FLAG MYC
MUNC18-1-145Y-A	PEGFP-N1	FLAG GFP
MUNC18-1-145Y-H	PEGFP-N1	FLAG GFP
MUNC18-1-145Y-E	PEGFP-N1	FLAG GFP
MUNC18-1-145Y-F	PEGFP-N1	FLAG GFP
FLAG-VAMP7-45Y-A	CMV10	FLAG
FLAG-VAMP7-45Y-C	CMV10	FLAG
FLAG-DYNAMIN2-125Y-A	pMYC-C2	FLAG MYC

FLAG-DYNAMIN2-125Y-E	pMYC-C2	FLAG	MYC
FLAG-DYNAMIN2-125Y-F	pMYC-C2	FLAG	MYC
His-DYNAMIN2	pET-28a	His	
His-DYNAMIN2-125Y-E	pET-28a	His	
His-DYNAMIN2-125Y-F	pET-28a	His	
SNAP25-101Y-A	PEGFP-N1	FLAG	GFP
PCDH-MUNC18-1-WT	PCDH	GFP	
PCDH-MUNC18-1-145Y-A	PCDH	GFP	
PCDH-MUNC18-1-145Y-H	PCDH	GFP	
PCDH-MUNC18-1-145Y-E	PCDH	GFP	
PCDH-MUNC18-1-145Y-F	PCDH	GFP	
His-MUNC18-1-WT	Pet15b	His	
His-MUNC18-1-145Y-H	Pet15b	His	
His-MUNC18-1-145Y-E	Pet15b	His	
His-MUNC18-1-145Y-F	Pet15b	His	
SYNTAXIN1	PEGFP-N1	FLAG	GFP
PCDH-DYNAMIN2-WT	PCDH	GFP	
PCDH-DYNAMIN2-125Y-E	PCDH	GFP	
PCDH-DYNAMIN2-125Y-F	PCDH	GFP	

Appendix Table S8. Primer sequence

Plasmid	Primer sequence
His-PTPMEG2-333Y-A	F:5'GAAACCTAGAGAAAAACCGTGCGGGGGATGTACCCTGCCTGGAC 3' R:5'GTCCAGGCAGGGTACATCCCCCGCACGGTTTTTCTCTAGGTTTC 3'
His-PTPMEG2-334G-R	F: 5' CTAGAGAAAAACCGTTATCGTGATGTACCCTGCCTGGAC 3' R: 5' GTCCAGGCAGGGTACATCACGATAACGGTTTTTCTCTAG 3'
His-PTPMEG2-335D-A	F: 5' GAAAAACCGTTATGGGGCGGTACCCTGCCTGGACC 3' R: 5' GGTCCAGGCAGGGTACCGCCCCATAACGGTTTTTC 3'
His-PTPMEG2-471Y-A	F: 5' AGTTCTTGAGCTGGCCAGACGCGGGTGTCCCTTCCTCA 3' R: 5' TGAGGAAGGGACACCCGCGTCTGGCCAGCTCAAGAACT 3'
His-PTPMEG2-471Y-F	F: 5' GCTGGCCAGACTTTGGTGTCCCTTC 3' R: 5' GAAGGGACACCAAAGTCTGGCCAGC 3'
His-PTPMEG2-519I-A	F: 5' ATTGCAGTGCAGGCGCGGGCAGGACAGGT 3' R: 5' ACCTGTCCTGCCCGCGCCTGCACTGCAAT 3'
His-PTPMEG2-559Q-A	F: 5' AGAGGGCCTTCAGCATCGCGACCCCTGAGCAGTACTA 3' R: 5' TAGTACTGCTCAGGGGTCGCGATGCTGAAGGCCCTCT 3'
PCDH-PTPMEG2	F: 5' CCATAGAAGATTCTAGAATGGAGCCCGCGACC 3' R: 5' CGTCGACTGCAGAATTCTTACAGATCCTCTTC 3'
MUNC18-1-GFP-145Y-H	F:5'TTCTCCCCTATGAGTCCCAGGTGCATTCCCTGGACTCCGCTGACTC T 3' R:5'AGAGTCAGCGGAGTCCAGGGAATGCACCTGGGACTCATAGGGGA GAA 3'
MUNC18-1-GFP-145Y-A	F:5'TCTCCCCTATGAGTCCCAGGTGGCTTCCCTGGACTCCGCTGACTCT T 3' R:5'AAGAGTCAGCGGAGTCCAGGGAAGCCACCTGGGACTCATAGGGG AGA 3'
GST-MUNC18-1-145Y-H	F:5'TCCAAAATCGGATCTGGTTCCGCGTGGATCCATGGATTACAAGGAT GACGACGATA 3' R:5'CGAGGCAGATCGTCAGTCAGTCACGATGCGGCCGCTCACTCCATT GTTGGAGCCTGATCCTCAAA 3'
GST-MUNC18-1-145Y-E	F:5'TCTCCCCTATGAGTCCCAGGTGGAGTCCCTGGACTCCGCTGACTCT TTCC 3' R:5'GTCAGCGGAGTCCAGGGACTCCACCTGGGACTCATAGGGGAGAA ACGC 3'
GST-MUNC18-1-145Y-F	F:5'TCTCCCCTATGAGTCCCAGGTGTTTTCCCTGGACTCCGCTGACTCTTT 3' F:5'GAAAGAGTCAGCGGAGTCCAGGGAAAACACCTGGGACTCATAGG

	GG 3'
FLAG-VAMP7-45Y-A	F: 5' CTGAAAATAATAAACTAACTGCCTCACATGGCAATTATTTGT 3' R: 5' ACAAATAATTGCCATGTGAGGCAGTTAGTTTATTATTTTCAG 3'
FLAG-VAMP7-45Y-C	F: 5' CTGAAAATAATAAACTAACTTGCTCACATGGCAATTATTTG 3' R: 5' CAAATAATTGCCATGTGAGCAAGTTAGTTTATTATTTTCAG 3'
FLAG-MYC-DYNAMIN2	F:5'TAGCAAGATCTCGAGCTCAAGCTTCGAATTCGATTACAAGGACGACG ATGACAAGATGGGCAACCGCGGGATGGAAGAGCTCATC 3' R:5'CGGTGGATCCCGGGCCCGCGGTACCGTCGACCTAGTCGAGCAGGG ACGGC 3'
FLAG-MYC-DYNAMIN2--125Y-A	F:5'GGTGCTCGAGTGCGGCCGCAAGCTTGTCGACCTAGTCGAGCAGGGA CGGCTC 3' R:5'GAGGGTCAAGTTCAACACGTGTGGTGAGGCGACCCGAAGGTTGA TGGGCACAGG 3'
FLAG-MYC-DYNAMIN2-RFP-125Y-E	F:5'TGCCCATCAACCTTCGGGTCGAGTCACCACACGTGTTGAACTTGA C 3' R:5'CAGCTGCCGGTAATCCTTAGCGACATTCCTCTGCTCAGTGTTGAA 3'
FLAG-MYC-DYNAMIN2-RFP-125Y-F	F:5'TGCCCATCAACCTTCGGGTCTTCTCACCACACGTGTTGAACTTGAC 3' R:5'TCAAGTTCAACACGTGTGGTGAGAAGACCCGAAGGTTGATGGGC ACAGG 3'
His-DYNAMIN2	F:5'CCCTGTGCCCATCAACCTTCGGGTCTACTCACCACACGTGTTGAAC TTGACC 3' R:5'GGTCAAGTTCAACACGTGTGGTGAGTAGACCCGAAGGTTGATGGG CACAGGG 3'
His-DYNAMIN2-125Y-E	F:5'CAGCGGCCTGGTGCCGCGCGGCAGCCATATGGGCAACCGCGGGAT GGAAGAGCTC 3' R:5'GGTGCTCGAGTGCGGCCGCAAGCTTGTCGACCTAGTCGAGCAGGG ACGGCT 3'
His-DYNAMIN2-125Y-F	F:5'CAGCGGCCTGGTGCCGCGCGGCAGCCATATGGGCAACCGCGGGAT GGAAGAGCTCA 3' R:5'GGTGCTCGAGTGCGGCCGCAAGCTTGTCGACCTAGTCGAGCAGGG ACGGCTC 3'
SNAP25-101Y-A	F:5'TCGCCACCATGGATTACAAGGATGACGACGATAAGATGGCCGAGGA CGCAGACATGCGTA 3' R:5'TACGCATGTCTGCGTCCTCGGCCATCTTATCGTCGTCATCCTTGTAA TCCATGGTGGCGA 3'

Q-rtPCR Primer sequence	
PTP-MEG2	F:5' AGTTTGATGTGCTCCGTGC 3' R:5' AGAGGGCAATGGAGGCTCC 3'
MUNC18-1	F: 5' TGGAAGGTGCTGGTGGTGGA 3' R: 5' GCAGTCGGCGGGTCCTTAA 3'

DYNAMIN2	F: 5' TTCGGTGCTCGAGAACTTCG 3' R: 5' CTCTGCTTCGATCTCCTGCC 3'
β -ACTIN	F: 5' AGGGCTATGCTCTCCCTCAC 3' R: 5' CTCTCAGCTGTGGTGGTGAA 3'